

#### Malaysian Journal of Mathematical Sciences

Journal homepage: https://mjms.upm.edu.my



# Analysis of Blood Flow With Nanoparticles Through A Porous Inclined Overlapping Stenosed Artery Under the Influence of External Magnetic Field

Satwai, N.  $^{\bullet *1,2}$ , Prasad, K. M.  $^{\bullet 1}$ , and Phani Kumari, M. V.  $^{\bullet 1}$ 

<sup>1</sup>Department of Mathematics, School of Science, GITAM (Deemed to be University), Hyderabad, Telangana State, India - 502329 <sup>2</sup>Department of Mathematics, B V Raju Institute of Technology, Vishnupur, Narsapur, Telangana State, India - 502313

E-mail: nsatwai@gitam.in \*Corresponding author

Received: 9 August 2024 Accepted: 15 January 2025

# **Abstract**

A mathematical model for a steady flow of blood mixed with nanoparticles through an inclined stenosed artery having porous wall under the influence of magnetic field was developed. Here, blood is treated as a micropolar fluid and stensosis is overlapped. The closed form expressions for blood flow characherisitcs namely velocity, temperature and concentration distribution are obtained by using Homotopy perturbation method (which is one the semi analytical method). The effects of various physical cahracteristics of fluid flow on the impedence (resistance) to the flow and wall shear stress are analysed graphically. A novel result was found that the resistance to the fluid flow increases with the heights of the stenosis. Variation in nature of blood flow is examined, for varying values of the permeability remains constant, Brownian motion parameter, angle of inclination, magnetic field intensity, and thermophoresis parameter. The study reveals that the shear stress decreases with the increase in intensity of magnetic field, but it decreases with increase in permeability parameter. The Steram lines are drawn to explore the flow pattern and characteristics of momentum transfer. This theoretical study will help to understanding the flow phenomenon in the stenosed (overlapping) arteries under magnetic and nanofluid influences, with potential applications in improving the design of biomedical devices and systems involving fluid flow in porous media.

**Keywords:** overlapping stenosis; flow resistance; pressure drop; wall shear stress; Brownian motion parameter; thermophoresis parameter.

# 1 Introduction

In the modern world, one of the most serious health risks is atherosclerosis, which is defined as the narrowing of the blood vessel lumen, or the inner open space or lumen of an artery, caused by fatty substance accumulation. This can lead to hypertension, myocardial infarction, and other problems. As a result, stenosis develops when abnormal and irregular growth disrupts regular blood circulation, and there is strong evidence that hydrodynamic parameters such as wall shear, flow resistance, and so on can all play a role in the development and evolution of this medical problem. Thus, a detailed understanding of the blood's flow field in a stenosed tube will aid in the accurate diagnosis and treatment of cardiovascular problems.

Given this, a number of authors have examined several mathematical models for fluid flow via stenosed/constricted channels [34, 16]. In all of these mathematical research findings, blood flow is defined as a fluid that is Newtonian [25]. However, Majhi and Nair [17] claimed that blood behaves like a non-newtonian fluid according to certain conditions. Shukla et al. [26] investigated non-Newtonian blood flow in an artery with mild stenosis and its effects on flow dynamics. Chaturani & Samy [7] studied pulsatile flow of casson's fluid through stenosed arteries with application to blood flow.

Micropolar fluid is a particular kind of non-newtonian fluid. Eringen [11] proposed the concept of micro-polar fluids in an effort to study the flow of non-newtonian fluids with microscopic effects caused by micro-rotational motion and spin inertia. Prasad and Yasa [23] investigated the micropolar fluid flow via a permeable artery using multiple stenoses. Charya [6] described the motion of blood as micropolar fluid flow with the objective to account for the micro spin of particles in suspension. This study investigates fluid circulation with continuous constrained borders in a non-symmetric vessel. Ellahi et al. [10] investigated micropolar fluid in composite arterial body fluid flow. Abdullah and Amin [1] developed a nonlinear two-dimensional micropolar fluid model to investigate blood flow in a tapering artery with stenosis. Mekheimer and Kot [19, 20] investigated the micropolar flow of fluid model for blood circulation in tapering stenosed veins.

Nanofluid is a fluid having nano meter sized particles known as nanoparticles. Nanofluids have been establish to possess enrich thermo physical properties like thermal diffusivity, thermal conductivity, convective heat transfer coefficients, including pharmaceutical processes, fuel cells, microelectronics and hybrid powered engine. Choi and Eastman [8] firstly introduced the investigation on the nanofluid. Recent blood flow models include nanoparticles, which can affect stenosed artery flow dynamics. Khan et al. [15] studied partial slip effects on peristaltic JS nanofluid flow with double-diffusive convection and an induced magnetic field. Yasmin et al. [33] examined peristaltic transport in different nanofluid models, and Bilal et al. [5] investigated double-diffusion convection and viscous dissipation on magneto-six-constant jeffrey nanofluids in biological fluid flow. These studies demonstrate the increasing significance of nano-fluid models in understanding challenging physiological processes and their medical consequences.

Magnetic fields have a critical role in the flow of blood inside the human vascular system. MHD applications reduce bodily fluid flow rate in human blood arteries while also helping in the treatment of certain cardiovascular disorders. Many magnetic devices have been developed for cancer treatment, cell separation, drug delivery, and other applications. In the presence of a magnetic field, substantial study on biofluid mechanics was conducted (Ikbal et al. [14]). Bali and Awasthi [4] examined the influence of an external transverse magnetic field on the flow of blood in a stenotic artery. Tanwar et al. [29] examined the impact of a porous medium and transverse magnetic field on blood flow in a stenosed artery and Varshney et al. [32] investigated a mathematical model to examine the impact of magnetic fields on blood circulation in arteries with multiple

stenotic regions. He [12, 13] investigated the application of homotopy perturbation.

The magnetic fields of newtonian and non-newtonian fluids have several applications in the fields of chemical engineering, biofluid mechanics, and other industries. A moving electrically conducting fluid will produce both electric and magnetic fields when exposed to a magnetic field. A body force called the Lorentz force is created when these fields interact, and it tends to oppose the liquid's movement (Craig and Watson [9]). Sud et al. [28] investigated how a moving magnetic field affected blood flow, they found that a suitable moving magnetic field accelerated blood flow. They identified that the magnetic field's impact can be used as a blood pump during cardiac procedures to improve blood flow in arteries with arterial disorders such as stenosis of the arteries or arteriosclerosis. Misra et al. [21] constructed a mathematical model to investigate blood flow through a porous vessel exhibiting multiple stenoses in the presence of an external magnetic field.

The influence of a porous medium on fluid flow is important because of its applications, which include fluid filtration, water flow in river beds, surface water and oil transport, physiological fluid flow in the bile duct, and blood flow through tiny arteries. These uses prompted other researchers to investigate flow dynamics in various geometries over porous media (Sochi [27]). The study conducted by Prasad and Yasa [24] examined the impact of slip on on the flow of a nanofluid via a duct that is inclined tapering stenosed artery having permeable borders. Zeeshan et al. [35] investigated the flow of copper-suspended nanofluid through a composite stenosed artery with permeable walls. The study conducted by Akbar et al. [2] examined the movement of nanofluid in a narrowing artery with porous walls [30]. Mandal [18] examined non-Newtonian blood flow in tapered arteries with stenosis, emphasizing the effects of tapering, wall motion, and the severity of stenosis. Azmi et al. [3] studied fractional Casson fluid flow in small arteries, highlighting the impact of slip conditions and cholesterol porosity on blood flow dynamics.

Many arteries in physiological processes are not horizontal, but rather angled toward the axis. Vajravelu et al. [31] investigated the Herschel-Bulkley fluid's peristaltic movement in an inclined tube. Studying the effect of the Herschel-Bulkley model, an explanation for non-newtonian fluid flow in tubes with multiple stenoses, could thus provide illumination on the role of fluid dynamical characteristics in the development and treatment of cardiovascular disease. Many researchers describe the stenosis as mild and single, while in reality, the stenosis is overlapping and irregularly shaped.

This study's innovative approach to modelling blood flow through an inclined overlapping stenosed artery treats blood as a micropolar fluid, including complex characteristics such as microrotational motion and spin inertia. This varies from conventional models that treat blood as a Newtonian fluid and simplify geometry to linear or uniform shapes. The research is more relevant to cardiovascular diseases by adopting realistic conditions with inclined and overlapping stenoses. The addition of nanoparticles to the blood flow model develops medical uses like targeted drug delivery and hyperthermia treatment, while magnetic field effects relate magnetohydrodynamics (MHD) to blood circulation dynamics, possibly leading to new treatment methods. The Homotopy Perturbation method (HPM) for analytical solutions introduces an original mathematical framework and shows its efficacy in biomedical nonlinear fluid dynamics issues. This discovery greatly improves our understanding of blood flow dynamics in stenosed arteries and provides novel avenues for research and treatment.

Motivated from the above studies a mathematical model has been developed for fluid flow across an inclined overlapping stenosed artery with the effect of a magnetic field through a porous medium. Blood is considered as a micropolar fluid with nanoparticles.

# 2 Mathematical Formulation

A cylindrical coordinate system  $(r, \theta, z)$  with r=0 as the cylinder's axis of symmetry is explored, where the z-axis runs parallel to the artery's axis. Consider the flow of a micropolar fluid across an inclined artery with overlapping stenoses, characterized by fluid viscosity  $\mu$  and density  $\rho$ .

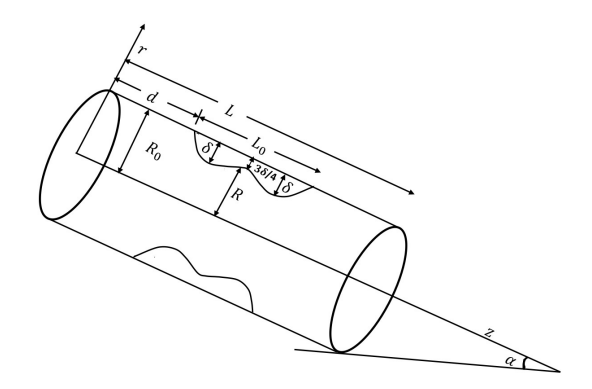


Figure 1: Schematic diagram of an inclined duct with overlapping stenoses.

Assuming the stenosis is to be mild and develops axially symmetrically . The cylindrical tube's radius is defined as,

$$h = \frac{R(z)}{R_0} = \begin{cases} 1 - \frac{3}{2} \frac{\delta}{R_0(L_0)^4} \left( 11(z - d)(L_0)^3 - 47(z - d)^2 (L_0)^2 + 72(z - d)^3 (L_0) - 36(z - d)^4 \right), & d \le z \le d + L_0, \\ 1, & \text{otherwise.} \end{cases}$$
(1)

The tube radius with narrowing is denoted by  $R\left(z\right)$ , while  $R_{0}(z)$  represents the tube radius without narrowing. The stenosis length is denoted by  $L_{0}$  and its location is represented by d. The maximum height of the stenoses situated at two locations z is denoted by  $\delta$ . The first location is  $z=d+\frac{L_{0}}{6}$ , and the second location is  $z=d+\frac{5L_{0}}{6}$ . The critical height is determined to be  $\frac{3\delta}{4}$  at  $z=d+\frac{L_{0}}{2}$ , measured from the origin. (Figure 1)

The mild stenosis approximation,  $\left(\frac{\delta}{R_0} \ll 1, Re\left(2\delta/L0\right) \ll 1 \text{ and } 2R_0/L_0\left(1\right)\right)$  are defined in Prasad et al. [22]. Accordingly, these are the governing equations for the fluid flow (Prasad et al. [24]):

$$\frac{\partial w_r}{\partial r} + \frac{w_r}{r} + \frac{\partial w_z}{\partial z} = 0, (2)$$

$$\rho\left(w_{r}\frac{\partial w_{z}}{\partial r} + w_{z}\frac{\partial w_{z}}{\partial z}\right) = -\frac{\partial p}{\partial z} + (\mu + K)\left(\frac{\partial^{2}w_{z}}{\partial r^{2}} + \frac{1}{r}\frac{\partial w_{z}}{\partial r} + \frac{\partial^{2}w_{z}}{\partial z^{2}}\right) + \frac{K}{r}\frac{\partial\left(rv_{\theta}\right)}{\partial r} + \frac{\sin\left[\alpha\right]}{F}$$

$$-\frac{\mu\bar{w}}{K} + \left(\bar{J}\times\bar{B}\right), \tag{3}$$

$$\rho\left(w_r\frac{\partial w_r}{\partial r}+w_z\cdot\frac{\partial w_r}{\partial z}\right)=-\frac{\partial p}{\partial r}+(\mu+K)\left(\frac{\partial^2 w_r}{\partial r^2}+\frac{1}{r}\frac{\partial w_r}{\partial r}-\frac{w_r}{r^2}\right)-\frac{\cos\left[\alpha\right]}{F}-K\frac{\partial v_\theta}{\partial z}, \tag{4}$$

$$\rho j \left( w_r \frac{\partial v_\theta}{\partial r} + w_z \frac{\partial v_\theta}{\partial z} \right) = -2Kv_\theta - K \left( \frac{\partial w_z}{\partial r} - \frac{\partial w_r}{\partial z} \right) + \gamma \left( \frac{\partial}{\partial r} \left( \frac{1}{r} \frac{\partial (rv_\theta)}{\partial r} \right) + \frac{\partial^2 v_\theta}{\partial z^2} \right). \tag{5}$$

Here, p,  $\rho$ , j, K,  $\mu$ , F, are fluid pressure, velocity vector, micro rotation vector, fluid density, micro gyration parameter, porous medium's permeability, viscocity, body force respectively.  $\bar{J} \times \bar{B}$  is lorentz force term in magnetohydrodynamics(  $\bar{J}$ : current density vector and  $\bar{B}$ : magnetic field vector).

Here,  $W=(w_r,\ 0,\ w_z)$  and  $V=(0,v_\theta,0)$  are respectively the velocity and microrotation vectors. The non-dimensional variables are:

$$\begin{split} \bar{\delta} &= \frac{\delta}{R_0}, \bar{z} = \frac{z}{L}, \bar{r} = \frac{r}{R_0}, \bar{w}_z = \frac{w_z}{w_0}, \bar{w}_r = \frac{Lw_r}{w_0\delta}, \; \bar{w}_\theta = \frac{R_0\vartheta_\theta}{w_0}, \bar{J} = \frac{j}{R_0^2}, \bar{p} = \frac{P}{\underline{\mu w_0 L}}, \; \bar{q} = \frac{q}{\pi R_0^2 w}, \\ R_e &= \frac{2\rho c_1 R_0}{\mu}, \quad F = \frac{\mu U^h}{\rho g \; R_0^{h+1}}, \quad N_b = \frac{(\rho c)_p \; D_{\bar{B}} \bar{C}_0}{(\rho c)_f}, \quad N_t = \frac{(\rho c)_p \; D_T \bar{T}_0}{(\rho c)_f \; \beta}, \quad G_r = \frac{g \beta \bar{T}_0 R_0^3}{\gamma^2}, \\ B_r &= \frac{g \beta \bar{C}_0 R_0^3}{\gamma^2}, \quad \theta_t = \frac{T - \bar{T}_0}{\bar{T}_0}, \quad \sigma = \frac{C - \bar{C}_0}{\bar{C}_0}, \quad \bar{F} = \frac{F}{\mu W \lambda'}, \quad M = \frac{\sigma R_0^2 B_0^2}{\rho \vartheta}. \end{split}$$

Apply the mild stenosis approximation,  $\left(\frac{\delta}{R_0} \ll 1, Re\left(2\delta/L0\right) \ll 1 \text{ and } 2R_0/L_0\left(1\right)\right)$  defined in Prasad et al. [22]. Hence, (2)-(5) becomes,

$$\frac{\partial P}{\partial r} = -\frac{\sin\left(\alpha\right)}{F},\tag{6}$$

$$\frac{N}{r}\frac{\partial}{\partial r}(rV_{\theta}) + \frac{\partial^{2}w}{\partial r^{2}} + \frac{1}{r}\frac{\partial w}{\partial r} + (1 - N)\frac{\sin\left[\alpha\right]}{F} + (1 - N)\left(G_{r}\theta + B_{r}\sigma\right) - \frac{\mu w}{k} - Mw = (1 - N)\frac{\partial P}{\partial z},$$
(7)

$$2V_{\theta} + \frac{\partial w}{\partial r} - \frac{2 - N}{m^2} \frac{\partial}{\partial r} \left( \frac{1}{r} \frac{\partial}{\partial r} \left( rV_{\theta} \right) \right) = 0, \tag{8}$$

$$\frac{1}{r}\frac{\partial}{\partial r}\left(r\frac{\partial\theta}{\partial r}\right) + N_b\frac{\partial\sigma}{\partial r}\frac{\partial\theta}{\partial r} + N_t\left(\frac{\partial\theta}{\partial r}\right)^2 = 0,\tag{9}$$

$$\frac{1}{r}\frac{\partial}{\partial r}\left(r\frac{\partial\sigma}{\partial r}\right) + \frac{N_t}{N_b}\left(\frac{1}{r}\frac{\partial}{\partial r}\left(r\frac{\partial\theta}{\partial r}\right)\right) = 0. \tag{10}$$

The axial velocity, denoted by w, has a radius of  $R_0$ . The temperature profile, nanoparticle phenomena, local temperature, and local nanoparticle Grashof numbers, Brownian motion number, Thermophoresis parameter, micropolar parameter and coupling number are represented by  $\theta$ ,  $\sigma$ ,  $B_r$ ,  $G_r$ ,  $N_b$ ,  $N_t$ , m and N. Additionally,  $M = \sigma B_0^2$  is the magnetic parameter,  $\mu$  is the viscosity, and k is the porous medium's permeability.

The following are the non-Dimensional boundary conditions:

$$w = 0,$$
  $V_{\theta} = 0,$   $\theta = 0,$  at  $r = h(z),$  (11)

$$\frac{\partial w}{\partial r} = 0,$$
  $\frac{\partial \theta}{\partial r} = 0,$   $\frac{\partial \sigma}{\partial r} = 0,$  at  $r = 0,$  (12)

$$V_{\theta}$$
 is finite at  $r = h(z)$ . (13)

## 3 Method of Solution

The solution of the coupled (9) and (10) have been calculated by the Homotopy perturbation method (HPM) as [23],

$$H(q,\theta) = (1-q)\left[L(\theta) - L(\theta_{10})\right] + q\left[L(\theta) + N_b \frac{\partial \sigma}{\partial r} \cdot \frac{\partial \theta}{\partial r} + N_t \left(\frac{\partial \theta}{\partial r}\right)^2\right],\tag{14}$$

$$H(q,\theta) = L(\theta) - L(\theta_{10}) + qL(\theta_{10}) + q\left[N_b \frac{\partial \sigma}{\partial r} \cdot \frac{\partial \theta}{\partial r} + N_t \left(\frac{\partial \theta}{\partial r}\right)^2\right], \tag{15}$$

$$H(q,\sigma) = (1-q)\left[L(\sigma) - L(\sigma_{10})\right] + q\left[L(\sigma) + \frac{N_t}{N_b}\left(\frac{1}{r}\frac{\partial}{\partial r}\left(r\frac{\partial\theta}{\partial r}\right)\right)\right],\tag{16}$$

$$H(q,\sigma) = L(\sigma) - L(\sigma_{10}) + qL(\sigma_{10}) + q\left[\frac{N_t}{N_b}\left(\frac{1}{r}\frac{\partial}{\partial r}\left(r\frac{\partial\theta}{\partial r}\right)\right)\right],\tag{17}$$

where the embedding parameter q is defined as,

$$0 \le q \le 1$$
.

The linear operator L is given by,

$$L \equiv \frac{1}{r} \frac{\partial}{\partial r} \left( r \cdot \frac{\partial}{\partial r} \right), \quad \theta_0 \left( r, z \right) = \left( \frac{r^2 - h^2}{4} \right), \quad \sigma_0 \left( r, z \right) = -\left( \frac{r^2 - h^2}{4} \right). \tag{18}$$

Define,

$$\theta(r,z) = \theta_0 + q\theta_1 + q^2\theta_2 + \dots,$$
 (19)

$$\sigma(r,z) = \sigma_0 + q\sigma_1 + q^2\sigma_2 + \dots$$
 (20)

Convergence of (19) and (20) depend on the non-linear part of the expression. Adopting the same procedure as done by (27), the solution for temperature profile ( $\theta$ ) and nanoparticle phenomenon ( $\sigma$ ) for q = 1 are,

$$\theta(r,z) = \frac{1}{64} (N_b - N_t) (r^2 - h^2) - \left(\frac{1}{18} N_b (r^3 - h^3) + \frac{N_t}{36864} (N_b^2 + N_t^2) (r^4 - h^4) (r^6 - h^6)\right), \tag{21}$$

$$\sigma(r,z) = \frac{-1}{4} \left( r^2 - h^2 \right) \frac{N_t}{N_b} + \frac{N_t}{N_b} \left( \frac{1}{18} N_b \left( r^3 - h^3 \right) + \frac{1}{36864} \left( N_b^2 + N_t^2 \right) \left( r^6 - h^6 \right) \right). \tag{22}$$

Substituting (21) and (22) in (7), and applying boundary conditions,

$$\frac{\partial}{\partial r} \left[ NrV_{\theta} + r \frac{\partial w}{\partial r} + \frac{(N-1)}{2} r^{2} \frac{dP}{dz} \right] 
= -(1-N) r \frac{\sin{[\alpha]}}{F} - (1-N) \left[ G_{r} \left( \frac{1}{64} \left( N_{b} - N_{t} \right) \left( r^{2} - h^{2} \right) - \left( \frac{1}{18} N_{b} \left( r^{3} - h^{3} \right) \right) \right] 
+ \frac{N_{t}}{36864} \left( N_{b}^{2} + N_{t}^{2} \right) \left( r^{4} - h^{4} \right) \left( r^{6} - h^{6} \right) \right) + B_{r} \left( \frac{-1}{4} \left( r^{2} - h^{2} \right) \frac{N_{t}}{N_{b}} + \frac{N_{t}}{N_{b}} \left( \frac{1}{18} N_{b} \left( r^{3} - h^{3} \right) \right) \right] 
+ \frac{1}{36864} \left( N_{b}^{2} + N_{t}^{2} \right) \left( r^{6} - h^{6} \right) \right) + \left( \frac{\mu}{k} + M \right) wr.$$
(23)

From (21), (22) and (8), expression for  $V_{\theta}$  can be written as,

$$\frac{\partial^{2} V_{\theta}}{\partial r^{2}} + \frac{1}{r} \frac{\partial V_{\theta}}{\partial r} - \left(m^{2} + \frac{1}{r^{2}}\right) V_{\theta}$$

$$= \frac{(1 - N) m^{2}}{(2 - N)} \left[ \frac{r}{2} \frac{dp}{dz} - \frac{r}{2} \frac{\sin{[\alpha]}}{F} \right] - \frac{(1 - N) m^{2}}{(2 - N)} \left[ G_{r} \left( \frac{1}{64} \left( N_{b} - N_{t} \right) \left( \frac{r^{3}}{4} - \frac{h^{2}r}{2} \right) \right) - \left( \frac{1}{18} N_{b} \left( \frac{r^{4}}{5} - \frac{h^{3}r}{2} \right) + \frac{N_{t} \left( N_{t}^{2} + N_{b}^{2} \right)}{36864} \left( \frac{r^{11}}{12} - \frac{r^{5}h^{6}}{6} - \frac{r^{7}h^{4}}{8} + \frac{rh^{10}}{2} \right) \right) \right) + B_{r} \left( \frac{-1}{4} \left( \frac{r^{3}}{4} - \frac{h^{2}r}{2} \right) \frac{N_{t}}{N_{b}} + \frac{N_{t}}{N_{b}} \left( \frac{N_{b}}{18} \left( \frac{r^{4}}{5} - \frac{h^{3}r^{2}}{2} \right) + \frac{\left( N_{b}^{2} + N_{t}^{2} \right)}{36864} \left( \frac{r^{7}}{8} - \frac{h^{6}r}{2} \right) \right) \right) \right] + \left( \frac{\mu}{k} + M \right) \frac{wr(m^{2})}{2(2 - N)}. \tag{24}$$

From (24),  $V_{\theta}$  is,

$$V_{\theta} = C_{2}(z) I_{1}(mr) + C_{3}(z) K_{1}(mr) - \frac{(1-N)r}{2(2-N)} \left(\frac{dP}{dz} - \frac{\sin{[\alpha]}}{F}\right) + \left(\frac{1-N}{2-N}\right) \times \left[G_{r}(N_{b} - N_{t}) \left(\frac{r}{32m^{2}} - \frac{h^{2}r}{128} + \frac{r^{3}}{256}\right) - G_{r}N_{b} \left(\frac{1}{2m^{4}} - \frac{rh^{3}}{36} + \frac{r^{2}}{6m^{2}} + \frac{r^{4}}{90}\right) - \frac{G_{r}N_{t}\left(N_{b}^{2} + N_{t}^{2}\right)}{36864} \left(\left(\frac{7372800r}{m^{10}} - \frac{1152h^{4}r}{m^{6}} - \frac{32h^{6}r}{m^{4}} + \frac{h^{10}r}{2} + \frac{921600r^{3}}{m^{8}} - \frac{144h^{4}r^{3}}{m^{4}} - \frac{4h^{6}r^{3}}{m^{2}} + \frac{38400r^{5}}{m^{6}} - \frac{6h^{4}r^{5}}{m^{2}} - \frac{h^{6}r^{5}}{6}\right) + \left(\frac{800r^{7}}{m^{4}} - \frac{h^{4}r^{7}}{8} + \frac{10r^{9}}{m^{2}} + \frac{r^{11}}{12}\right) - \frac{B_{r}N_{t}}{N_{b}} \times \left(\frac{r}{2m^{2}} - \frac{rh^{2}}{8} + \frac{r^{3}}{16}\right) + B_{r}N_{t}\left(\frac{1}{2m^{4}} - \frac{rh^{3}}{36} + \frac{r^{2}}{6m^{2}} + \frac{r^{4}}{90}\right) + \left(\frac{N_{t}}{N_{b}}\right) \frac{B_{r}\left(N_{b}^{2} + N_{t}^{2}\right)}{36864} \times \left(\frac{1152r}{m^{6}} - \frac{h^{6}r}{2} + \frac{144r^{3}}{m^{4}} + \frac{6r^{5}}{m^{2}} + \frac{r^{7}}{8}\right) - \frac{wr}{2(2-N)}\left(\frac{\mu}{k} + M\right)\right],$$
(25)

where  $I_1(mr)$  and  $K_1(mr)$  are respectively the first and second order modified Bessel functions. Substitute (25) in (23), and by applying boundary conditions (11)-(13), the velocity is,

$$w\left[z,r\right] = \frac{1}{\left[1 - \left(\frac{\mu}{k} + M\right) \frac{r^2}{2\left(2 - N\right)}\right]} \left[ -NC_2\left(z\right) \frac{I_0\left(mr\right)}{m} + \frac{\left(1 - N\right)r^2}{\left(2 - N\right)} \frac{r^2}{2} \left(\frac{dP}{dz} - \frac{\sin\left[\alpha\right]}{F}\right) - \frac{\left(1 - N\right)r^2}{\left(2 - N\right)} \right] \\ \times \left(G_r\left(N_b - N_t\right) \left(\frac{Nr^2}{64m^2} + \frac{r^4}{512} - \frac{r^2h^2}{128}\right) - G_rN_b \left(\frac{Nr}{2m^4} + \frac{Nr^3}{18m^2} + \frac{r^5}{225} - \frac{r^2h^2}{36}\right) \times \\ \left( -\frac{G_rN_t\left(N_b^2 + N_t^2\right)}{36864} \left(\frac{7372800Nr^2}{2m^{10}} + \frac{230400Nr^4}{m^8} - \frac{576Nr^2h^2}{m^6} + \frac{6400Nr^6}{m^6} - \frac{16h^6Nr^2}{m^4} \right) \right. \\ \left. - \frac{36h^4r^4}{m^4} + \frac{100Nr^8}{m^4} - \frac{Nh^6r^4}{m^2}\right) + \left(\frac{Nr^{10}}{m^2} - \frac{Nh^4r^6}{m^2} + \frac{r^{12}}{72} - \frac{r^6h^6}{18} - \frac{r^8h^4}{32} + \frac{r^2h^{10}}{2}\right) \right) \\ - \frac{B_rN_t}{N_b} \left(\frac{Nr^2}{4m^2} + \frac{r^4}{32} - \frac{r^2h^2}{8}\right) + B_rN_t \left(\frac{Nr}{2m^4} + \frac{Nr^3}{18m^2} + \frac{r^5}{225} - \frac{r^2h^3}{36}\right) \\ + \frac{B_r\left(N_t^2 + N_b^2\right)}{36864} \frac{Nt}{Nb} \left(\frac{576Nr^2}{m^6} + \frac{36Nr^4}{m^4} + \frac{Nr^6}{m^2} - \frac{r^8}{32} - \frac{h^6r^2}{2}\right) \right) + C_4 \right], \tag{26}$$

(27)

where

$$\begin{split} C_4 &= NC_2 \frac{I_0 \left(mh\right)}{m} - \frac{\left(1-N\right)}{\left(2-N\right)} \frac{h^2}{q} \left(\frac{dP}{dz} - \frac{\sin\left[\alpha\right]}{F}\right) + \frac{\left(1-N\right)}{\left(2-N\right)} \left(G_r \left(N_b - N_t\right) \left(\frac{Nh^2}{64m^2} - \frac{3h^4}{512}\right) \right. \\ &- G_r N_b \left(\frac{Nh}{2m^4} + \frac{Nh^3}{18m^2} - \frac{7h^5}{300}\right) - \frac{B_r N_t}{Nb} \left(\frac{Nh^2}{4m^2} - \frac{3h^4}{8}\right) + B_r N_t \left(\frac{Nh}{2m^4} + \frac{Nh^3}{18m^2} - \frac{7h^5}{300}\right) \\ &- \frac{G_r N_t \left(N_b^2 + N_t^2\right)}{36864} \left(\frac{3686400Nh^2}{m^{10}} + \frac{230400Nh^4}{m^{10}} + \frac{5824Nh^6}{m^6} + \frac{48Nh^8}{m^4} - \frac{Nh'^0}{m^2} + \frac{41h^{12}}{96}\right) \\ &+ \frac{B_r \left(N_t^2 + N_b^2\right)}{36864} \frac{Nt}{Nb} \left(\frac{576Nh^2}{m^6} + \frac{36Nh^4}{m^4} + \frac{Nh^6}{m^2} - \frac{15h^8}{32}\right)\right), \\ C_2 &= \frac{1}{I_1 \left(mh\right)} \left[\frac{\left(1-N\right)}{\left(2-N\right)} \left(\frac{dP}{dz} - \frac{\sin\left[\alpha\right]}{F}\right) \frac{h}{2} - \frac{\left(1-N\right)}{\left(2-N\right)} \left(G_r \left(N_b - N_t\right) \left(\frac{h}{2m^2} - \frac{h^3}{256}\right) - G_r N_b \right. \\ &\times \left(\frac{1}{2m^4} + \frac{h^2}{6m^2} - \frac{h^4}{60}\right) - \frac{G_r N_b \left(N_b^2 + N_t^2\right)}{36864} \left(\frac{7372800h}{m^{10}} + \frac{921600h^3}{m^8} + \frac{37248h^5}{m^6} + \frac{624h^7}{m^4} \right. \\ &+ \frac{7h^{11}}{24} - \frac{B_r N_t}{N_b} \left(\frac{h}{2m^2} - \frac{h^3}{16}\right) + B_r N_t \left(\frac{1}{2m^4} + \frac{h^2}{6m^2} - \frac{h^4}{60}\right) + \frac{B_r \left(N_b^2 + N_t^v\right)}{36864} \frac{N_t}{N_b} \times \\ &\left(\frac{1152h}{m^6} + \frac{144h^3}{m^4} + \frac{6h^5}{m^2} - \frac{3h^7}{8}\right)\right) \right]. \end{split}$$

Dimension less flux(q) can be determined as follows:

$$q = \int_{0}^{h} 2rw \, dr, \tag{27}$$

$$q = \left[ \left( \frac{Nh^{2}}{m} \frac{I_{0}(mh)}{I_{1}(mh)} - \frac{2Nh}{m} \right) + \frac{\left( \frac{\mu}{k} + M \right)}{(2-N)} \left( \frac{N}{m} \frac{I_{0}(mh)}{I_{1}(mh)} \frac{h^{4}}{4} - \frac{Nh^{3}}{m} + \frac{2Nh^{2}}{m} \frac{I_{2}(mh)}{I_{1}(mh)} \right) \left( \frac{(1-N)}{(2-N)} \right) \right]$$

$$\times \left( \frac{dP}{dz} - \frac{\sin{[\alpha]}}{F} \right) \frac{h}{2} - \frac{(1-N)}{(2-N)} \left( G_{r} \left( N_{b} - N_{t} \right) \left( \frac{h}{32m^{2}} - \frac{h^{3}}{256} \right) - G_{r} N_{b} \left( \frac{1}{2m^{4}} + \frac{h^{2}}{6m^{2}} - \frac{h^{4}}{60} \right) \right)$$

$$- \frac{G_{r} N_{t} \left( N_{b}^{2} + N_{t}^{2} \right)}{36864} \left( \frac{7372800h}{m^{10}} + \frac{37248h^{5}}{m^{6}} + \frac{624h^{7}}{4^{4}} + \frac{7h^{11}}{24} + \frac{921600h^{3}}{m^{8}} \right) - \frac{B_{r} N_{t}}{N_{b}} \left( \frac{h}{2m^{2}} \right)$$

$$- \frac{h^{3}}{16} \right) + B_{r} N_{t} \left( \frac{1}{2m^{4}} + \frac{h^{2}}{6m^{2}} - \frac{h^{4}}{60} \right) + \left( \frac{1152h}{m^{6}} + \frac{144h^{3}}{4^{4}} + \frac{6h^{5}}{m^{2}} - \frac{3h^{7}}{8} \right) \frac{B_{r} \left( N_{b}^{2} + N_{t}^{2} \right)}{36864} \times$$

$$\left( \frac{N_{t}}{N_{b}} \right) \right) \right] + \frac{(1-N)}{(2-N)} \left( \frac{-h^{4}}{4} - \frac{h^{6}}{24} \frac{\left( \frac{\mu}{k} + M \right)}{(2-N)} \right) \left( \frac{dP}{dz} - \frac{\sin{\alpha}}{r} \right) - \frac{(1-N)}{(2-N)} \left[ G_{r} \left( N_{b} - N_{t} \right) \times \right]$$

$$\left( \left( \frac{-Nh^{4}}{128m^{2}} + \frac{379h^{6}}{1536} \right) + \left( \frac{-Nh^{6}}{768m^{2}} + \frac{755h^{6}}{12288} \right) \frac{\left( \frac{\mu}{k} + M \right)}{(2-N)} \right) - G_{r} N_{b} \left( \left( -\frac{Nh^{3}}{6m^{4}} - \frac{Nh^{5}}{30m^{2}} + \frac{3h^{7}}{380} \right)$$

$$+ \left( \frac{-Nh^{5}}{40m^{4}} - \frac{Nh^{7}}{168m^{2}} + \frac{11h^{9}}{6480} \right) \frac{\left( \frac{\mu}{k} + M \right)}{(2-N)} - \frac{G_{r} N_{t} \left( N_{t}^{2} + N_{b}^{2} \right)}{36864} \left( \left( -\frac{1843200Nh^{4}}{m^{10}} - \frac{153600Nh^{6}}{m^{8}} \right)$$

$$- \frac{2255Nh^{8}}{m^{6}} - \frac{24Nh^{10}}{m^{4}} + \frac{7Nh^{12}}{24m^{2}} - \frac{73h^{14}}{210} \right) + \left( -\frac{307200Nh^{6}}{m^{10}} - \frac{28800Nh^{8}}{m^{8}} - \frac{912Nh^{6}}{m^{6}}$$

$$- \frac{65Nh^{12}}{6m^{4}} + \frac{27Nh^{14}}{280m^{2}} - \frac{59h^{16}}{1920} \right) \frac{\left( \frac{\mu}{k} + m \right)}{(2-N)} - \frac{B_{r}Nt}{N_{b}} \left( \left( -\frac{Nh^{4}}{8m^{2}} + \frac{31h^{4}}{192} \right) + \left( -\frac{Nh^{6}}{48m^{2}} + \frac{59h^{8}}{768} \right)$$

$$\times \frac{\left( \frac{\mu}{k} + M \right)}{(2-N)} + B_{r}Nt \left( \left( -\frac{Nh^{3}}{6m^{4}} - \frac{Nh^{5}}{30m^{2}} + \frac{3h^{7}}{380} \right) + \left( -\frac{Nh^{5}}{40m^{4}} - \frac{Nh^{5}}{168m^{2}} + \frac{11h^{9}}{64$$

$$+\frac{B_r\left(N_t^2+N_b^2\right)}{36864}\left(\frac{N_t}{N_b}\right)\left(\left(\frac{-288Nh^4}{m^6}-\frac{24Nh^6}{m^4}-\frac{3Nh^8}{4m^2}+\frac{19h^{10}}{80}\right)+\left(\frac{-48Nh^6}{m^6}-\frac{9Nh^8}{2m^4}-\frac{3Nh^{10}}{20m^2}+\frac{h^{12}}{32}\right)\frac{\left(\frac{\mu}{k}+M\right)}{(2-N)}\right)\right]. \tag{28}$$

From (28),  $\frac{dP}{dz}$  is,

$$\frac{dP}{dz} = \frac{\sin{[\alpha]}}{F} + \left[ \frac{1}{\left( \left( \frac{Nh^3}{2m} \frac{I_0(mh)}{I_1(mh)} - \frac{Nh^2}{m} - \frac{h^4}{4} \right) + \left( \frac{N}{m} * \frac{I_0(mh)}{I_1(mh)} \frac{h^5}{8} - \frac{Nh^4}{2m} - \frac{Nh^3}{m} * \frac{I_2(mh)}{I_1(mh)} - \frac{h^6}{24} \right) \left( \frac{\frac{\mu}{k} + M}{(2 - N)} \right)}{\left( \frac{\mu}{(1 - N)} + \left( \left( \frac{Nh^2}{2m} * \frac{I_0(mh)}{I_1(mh)} - \frac{2Nh}{m} \right) + \left( \frac{N}{m} * \frac{I_0(mh)}{I_1(mh)} \frac{h^4}{4} - \frac{Nh^3}{m} * \frac{I_2(mh)}{I_1(mh)} - \frac{h^6}{24} \right) \left( \frac{\frac{\mu}{k} + M}{I_1(mh)} \right)} \right] \times \left( \frac{\left( \frac{\mu}{k} + M \right)}{(2 - N)} \right) \left( G_r \left( N_b - N_t \right) \left( \frac{h}{32m^2} - \frac{h^3}{256} \right) - G_r N_b \left( \frac{1}{2m^4} + \frac{h^2}{6m^2} - \frac{h^4}{60} \right) \right) - \frac{G_r N_t \left( N_b^2 + N_t^2 \right)}{36864} \left( \frac{7372800h}{m^{10}} + \frac{37248h^5}{m^6} + \frac{624h^7}{m^4} + \frac{7h^{11}}{24} + \frac{921600h^3}{m^8} \right) - \frac{B_r N_t}{N_b} \times \left( \frac{h}{2m^2} - \frac{h^3}{6} \right) + B_r N_t \left( \frac{1}{2m^4} + \frac{h^2}{6m^2} - \frac{h^4}{60} \right) + \frac{B_r \left( N_b^2 + N_t^2 \right)}{36864} \left( \frac{N_t}{N_b} \right) \left( \frac{1152h}{m^6} + \frac{144h^3}{m^4} \right) + \frac{6h^5}{m^2} - \frac{3h^7}{8} \right) + \left( G_r \left( N_b - N_t \right) \left( \left( \frac{-Nh^4}{128m^2} + \frac{379h^6}{1536} \right) + \left( \frac{-Nh^6}{768m^2} + \frac{755h^6}{12288} \right) \frac{\left( \frac{\mu}{k} + M \right)}{(2 - N)} \right) - G_r N_b \left( \left( -\frac{Nh^3}{6m^4} - \frac{Nh^5}{30m^2} + \frac{3h^7}{280} \right) + \left( \frac{-Nh^4}{40m^4} - \frac{Nh^3}{168m^2} + \frac{11h^9}{4680} \right) \left( \frac{\left( \frac{\mu}{k} + M \right)}{(2 - N)} \right) - \frac{B_r N_t}{N_b} \times \left( \left( \frac{-Nh^4}{8m^2} + \frac{31h^4}{192} \right) + \left( \frac{-Nh^6}{48m^2} + \frac{59h^8}{768} \right) \left( \frac{\mu}{k} + M \right) - \frac{G_r N_t \left( N_t^2 + N_b^2 \right)}{36864} \left( \left( \frac{-1843200Nh^4}{m^{10}} \right) - \frac{153600Nh^6}{m^8} \right) + \frac{27Nh^4}{280m^2} + \frac{59h^{16}}{1920} \left( \frac{\mu}{k} + M \right) + \frac{B_r \left( N_t^2 + N_b^2 \right)}{36864} \left( \frac{N_t}{N_b} \right) \left( \left( \frac{-288Nh^4}{m^6} - \frac{24Nh^6}{m^6} \right) + \frac{3Nh^8}{4m^2} + \frac{11h^9}{80} \right) + \left( \frac{-28Nh^6}{6m^4} - \frac{3Nh^8}{6480} \right) \left( \frac{\mu}{k} + M \right) + \frac{3Nh^8}{36864} \left( \frac{N_t}{N_b} \right) \left( \frac{\mu}{k} + M \right) + \frac{N_t}{36864} \left( \frac{N_t}{N_b} \right) \left( \frac{-288Nh^4}{m^6} - \frac{24Nh^6}{m^6} \right) + \frac{3Nh^8}{36864} \left( \frac{N_t}{N_b} \right) \left( \frac{N_t}{k} \right) \left($$

The pressure drop per wave length  $\Delta p = p(0) - p(\lambda)$ ,

$$\Delta p = -\int_0^1 \frac{dP}{dz} \, dz,$$

$$\begin{split} \Delta p &= -\int_{0}^{1} \left[ \frac{\sin{[\alpha]}}{F} + \right. \\ &\left. \left( \frac{1}{\left( \left( \frac{Nh^{3}}{2m} \frac{I_{0}(mh)}{I_{1}(mh)} - \frac{Nh^{2}}{m} - \frac{h^{4}}{4} \right) + \left( \frac{N}{m} * \frac{I_{0}(mh)}{I_{1}(mh)} \frac{h^{5}}{8} - \frac{Nh^{4}}{2m} - \frac{Nh^{3}}{m} * \frac{I_{2}(mh)}{I_{1}(mh)} - \frac{h^{6}}{24} \right) \left( \frac{\frac{\mu}{\kappa} + M}{(2-N)} \right) \right) \right. \\ &\left. \left( \frac{q\left( 2 - N \right)}{(1 - N)} + \left( \left( \frac{Nh^{2}}{2m} * \frac{I_{0}\left( mh \right)}{I_{1}\left( mh \right)} - \frac{2Nh}{m} \right) + \left( \frac{N}{m} * \frac{I_{0}\left( mh \right)}{I_{1}\left( mh \right)} \frac{h^{4}}{4} - \frac{Nh^{3}}{m} - \frac{2Nh^{2}}{m} \frac{I_{2}\left( mh \right)}{I_{1}\left( mh \right)} \right) \times \right. \end{split}$$

$$\left( \frac{\binom{\mu}{k} + M}{(2 - N)} \right) \left( G_r \left( N_b - N_t \right) \left( \frac{h}{32m^2} - \frac{h^3}{256} \right) - G_r N_b \left( \frac{1}{2m^4} + \frac{h^2}{6m^2} - \frac{h^4}{60} \right) \right)$$

$$- \frac{G_r N_t \left( N_b^2 + N_t^2 \right)}{36864} \left( \frac{7372800h}{m^{10}} + \frac{37248h^5}{m^6} + \frac{624h^7}{m^4} + \frac{7h^{11}}{24} + \frac{921600h^3}{m^8} \right) - \frac{B_r N_t}{N_b} \times$$

$$\left( \frac{h}{2m^2} - \frac{h^3}{16} \right) + B_r N_t \left( \frac{1}{2m^4} + \frac{h^2}{6m^2} - \frac{h^4}{60} \right) + \frac{B_r \left( N_b^2 + N_t^2 \right)}{36864} \left( \frac{N_t}{N_b} \right) \left( \frac{1152h}{m^6} + \frac{144h^3}{m^4} \right)$$

$$+ \frac{6h^5}{m^2} - \frac{3h^7}{8} \right) + \left( G_r \left( N_b - N_t \right) \left( \left( \frac{-Nh^4}{128m^2} + \frac{379h^6}{1536} \right) + \left( \frac{-Nh^6}{768m^2} + \frac{755h^6}{12288} \right) \frac{\binom{\mu}{k} + M}{(2 - N)} \right)$$

$$- G_r N_b \left( \left( -\frac{Nh^3}{6m^4} - \frac{Nh^5}{30m^2} + \frac{3h^7}{280} \right) + \left( \frac{-Nh^5}{40m^4} - \frac{Nh^7}{168m^2} + \frac{11h^9}{6480} \right) \frac{\binom{\mu}{k} + M}{(2 - N)} \right) - \frac{B_r N t}{N_b} \times$$

$$\left( \left( \frac{-Nh^4}{8m^2} + \frac{31h^4}{192} \right) + \left( \frac{-Nh^6}{48m^2} + \frac{59h^8}{768} \right) \frac{\binom{\mu}{k} + M}{(2 - N)} \right) - \frac{G_r N_t \left( N_t^2 + N_b^2 \right)}{36864} \left( \left( \frac{-1843200Nh^4}{m^{10}} \right) \right)$$

$$- \frac{153600Nh^6}{m^8} - \frac{2255Nh^8}{m^6} - \frac{24Nh^{10}}{m^4} + \frac{7Nh^{12}}{24m^2} - \frac{73h^{14}}{210} \right) + \left( \frac{-307200Nh^6}{m^{10}} - \frac{28800Nh^8}{m^8} \right)$$

$$- \frac{912Nh^6}{m^6} - \frac{65Nh^{12}}{6m^4} + \frac{27Nh^{14}}{280m^2} - \frac{59h^{16}}{1920} \right) \frac{\binom{\mu}{k} + M}{(2 - N)} + B_r N_t \left( \left( -\frac{Nh^3}{6m^4} - \frac{Nh^5}{30m^2} + \frac{3h^7}{280} \right)$$

$$+ \left( \frac{-Nh^5}{40m^4} - \frac{Nh^7}{168m^2} + \frac{11h^9}{6480} \right) \frac{\binom{\mu}{k} + M}{(2 - N)} + \frac{B_r \left( N_t^2 + N_b^2 \right)}{36864} \left( \frac{N_t}{N_b} \right) \left( \left( \frac{-288Nh^4}{m^6} - \frac{24Nh^6}{m^4} \right)$$

$$- \frac{3Nh^8}{4m^2} + \frac{19h^{10}}{80} + \left( \frac{-48Nh^6}{6480} - \frac{9Nh^8}{2m^4} - \frac{3Nh^{10}}{20m^2} + \frac{h^{12}}{32} \right) \frac{\binom{\mu}{k} + M}{(2 - N)} \right) \right) dz.$$

Also, flow resistance  $\lambda$  is defined as,

$$\lambda = \frac{\Delta p}{a}$$

$$\begin{split} \lambda &= \frac{-1}{q} \int_0^1 \left[ \frac{\sin{[\alpha]}}{F} + \right. \\ &\left. \left( \frac{1}{\left( \left( \frac{Nh^3}{2m} \frac{I_0(mh)}{I_1(mh)} - \frac{Nh^2}{m} - \frac{h^4}{4} \right) + \left( \frac{N}{m} * \frac{I_0(mh)}{I_1(mh)} \frac{h^5}{8} - \frac{Nh^4}{2m} - \frac{Nh^3}{m} * \frac{I_2(mh)}{I_1(mh)} - \frac{h^6}{24} \right) \left( \frac{\frac{\mu}{\kappa} + M}{(2-N)} \right) \right) \times \\ &\left. \left( \frac{q \left( 2 - N \right)}{(1 - N)} + \left( \left( \frac{Nh^2}{2m} * \frac{I_0(mh)}{I_1(mh)} - \frac{2Nh}{m} \right) + \left( \frac{N}{m} * \frac{I_0(mh)}{I_1(mh)} \frac{h^4}{4} - \frac{Nh^3}{m} - \frac{2Nh^2}{m} \frac{I_2(mh)}{I_1(mh)} \right) \times \\ &\left. \left( \frac{\left( \frac{\mu}{\kappa} + M \right)}{(2 - N)} \right) \right) \left( G_r \left( N_b - N_t \right) \left( \frac{h}{32m^2} - \frac{h^3}{256} \right) - G_r N_b \left( \frac{1}{2m^4} + \frac{h^2}{6m^2} - \frac{h^4}{60} \right) \right. \\ &\left. - \frac{G_r N_t \left( N_b^2 + N_t^2 \right)}{36864} \left( \frac{7372800h}{m^{10}} + \frac{37248h^5}{m^6} + \frac{624h^7}{m^4} + \frac{7h^{11}}{24} + \frac{921600h^3}{m^8} \right) - \frac{B_r N_t}{N_b} \times \\ &\left. \left( \frac{h}{2m^2} - \frac{h^3}{16} \right) + B_r N_t \left( \frac{1}{2m^4} + \frac{h^2}{6m^2} - \frac{h^4}{60} \right) + \frac{B_r \left( N_b^2 + N_t^2 \right)}{36864} \left( \frac{N_t}{N_b} \right) \left( \frac{1152h}{m^6} + \frac{144h^3}{m^4} \right) \right. \\ &\left. + \frac{6h^5}{m^2} - \frac{3h^7}{8} \right) \right) + \left( G_r \left( N_b - N_t \right) \left( \left( \frac{-Nh^4}{128m^2} + \frac{379h^6}{1536} \right) + \left( \frac{-Nh^6}{768m^2} + \frac{755h^6}{12288} \right) \frac{\left( \frac{\mu}{k} + M \right)}{(2 - N)} \right) - \frac{B_r N_t}{N_b} \times \\ &\left. - G_r N_b \left( \left( - \frac{Nh^3}{6m^4} - \frac{Nh^5}{30m^2} + \frac{3h^7}{280} \right) + \left( \frac{-Nh^5}{40m^4} - \frac{Nh^7}{168m^2} + \frac{11h^9}{6480} \right) \frac{\left( \frac{\mu}{k} + M \right)}{(2 - N)} \right) - \frac{B_r N_t}{N_b} \right. \end{split}$$

$$\left( \left( \frac{-Nh^4}{8m^2} + \frac{31h^4}{192} \right) + \left( \frac{-Nh^6}{48m^2} + \frac{59h^8}{768} \right) \frac{\binom{\mu}{k} + M}{(2 - N)} \right) - \frac{G_r N_t \left( N_t^2 + N_b^2 \right)}{36864} \left( \left( \frac{-1843200Nh^4}{m^{10}} \right) \right)$$

$$- \frac{153600Nh^6}{m^8} - \frac{2255Nh^8}{m^6} - \frac{24Nh^{10}}{m^4} + \frac{7Nh^{12}}{24m^2} - \frac{73h^{14}}{210} \right) + \left( \frac{-307200Nh^6}{m^{10}} - \frac{28800Nh^8}{m^8} \right)$$

$$- \frac{912Nh^6}{m^6} - \frac{65Nh^{12}}{6m^4} + \frac{27Nh^{14}}{280m^2} - \frac{59h^{16}}{1920} \right) \frac{\binom{\mu}{k} + m}{(2 - N)} + B_r N_t \left( \left( -\frac{Nh^3}{6m^4} - \frac{Nh^5}{30m^2} + \frac{3h^7}{280} \right) \right)$$

$$+ \left( \frac{-Nh^5}{40m^4} - \frac{Nh^7}{168m^2} + \frac{11h^9}{6480} \right) \frac{\binom{\mu}{k} + M}{(2 - N)} + \frac{B_r \left( N_t^2 + N_b^2 \right)}{36864} \left( \frac{N_t}{N_b} \right) \left( \left( \frac{-288Nh^4}{m^6} - \frac{24Nh^6}{m^4} \right) \right)$$

$$- \frac{3Nh^8}{4m^2} + \frac{19h^{10}}{80} + \left( \frac{-48Nh^6}{m^6} - \frac{9Nh^8}{2m^4} - \frac{3Nh^{10}}{20m^2} + \frac{h^{12}}{32} \right) \frac{\binom{\mu}{k} + M}{(2 - N)} \right) \right) dz.$$

$$(31)$$

Equation  $\Delta p$  is used to calculate the pressure drop when there is no stenosis h=1, which is indicated by  $\Delta p_n$ ,

$$\begin{split} \Delta p_n &= -\int_0^1 \left[\frac{\sin\left[\alpha\right]}{F} + \left(\frac{1}{\left(\left(\frac{N}{2m}\frac{I_0(m)}{I_1(m)} - \frac{N}{m} - \frac{1}{4}\right) + \left(\frac{N}{m}\frac{I_0(m)}{I_1(m)}\frac{1}{8} - \frac{N}{2m} - \frac{N}{m}\frac{I_2(m)}{I_1(m)} - \frac{1}{24}\right) \left(\frac{\mu+M}{(2-N)}\right)\right)} \right) \times \\ & \left(\frac{q\left(2-N\right)}{\left(1-N\right)} + \left(\left(\frac{N}{2m}\frac{I_0(m)}{I_1(m)} - \frac{2N}{m}\right) + \left(\frac{N}{m}\frac{I_0(m)}{I_1(m)}\frac{1}{4} - \frac{N}{m} - \frac{2N}{m}\frac{I_2(m)}{I_1(m)}\right) \left(\frac{(\mu+M)}{(2-N)}\right)\right) \times \\ & \left(G_r\left(N_b-N_t\right) \left(\frac{1}{32m^2} - \frac{1}{256}\right) - G_rN_b\left(\frac{1}{2m^4} + \frac{1}{6m^2} - \frac{1}{60}\right) - \frac{G_rN_t\left(N_b^2 + N_t^2\right)}{36864} \times \right. \\ & \left(\frac{7372800}{m^{10}} + \frac{37248}{m^6} + \frac{624}{m^4} + \frac{7}{24} + \frac{921600}{m^8}\right) - \frac{B_rN_t}{N_b} \left(\frac{1}{2m^2} - \frac{1}{16}\right) + B_rN_t\left(\frac{1}{2m^4} + \frac{1}{6m^2}\right) - \frac{1}{6m^2} \right. \\ & \left(\frac{1}{2m^4} + \frac{1}{6m^2}\right) + \frac{B_r\left(N_b^2 + N_t^2\right)}{36864} \left(\frac{N_t}{N_b}\right) \left(\frac{1152}{m^6} + \frac{144}{m^4} + \frac{6}{m^2} - \frac{3}{8}\right)\right) + \left(G_r\left(N_b - N_t\right) \left(\left(\frac{-N}{128m^2}\right) + \frac{379}{1536}\right) + \left(\frac{-N}{768m^2} + \frac{755}{12288}\right) \frac{(\mu+M)}{(2-N)}\right) - G_rN_b\left(\left(-\frac{N}{6m^4} - \frac{N}{30m^2} + \frac{3}{280}\right) + \left(\frac{-N}{40m^4}\right) - \frac{N}{168m^2} + \frac{11}{6480}\right) \frac{(\mu+M)}{(2-N)}\right) - \frac{B_rNt}{N_b} \left(\left(\frac{-N}{8m^2} + \frac{31}{192}\right) + \left(\frac{-N}{48m^2} + \frac{59}{768}\right) \frac{(\mu+M)}{(2-N)}\right) - \frac{G_rN_t\left(N_t^2 + N_b^2\right)}{36864} \left(\left(\frac{-1843200N}{m^{10}} - \frac{153600N}{m^8} - \frac{2255N}{280m^2} - \frac{24N}{1920}\right) \frac{(\mu+M)}{(2-N)}\right) + B_rN_t \times \\ \left(\left(-\frac{N}{6m^4} - \frac{N}{30m^2} + \frac{3}{280}\right) + \left(\frac{-N}{40m^4} - \frac{N}{168m^2} + \frac{11}{6480}\right) \frac{(\mu+M)}{(2-N)}\right) + B_rN_t \times \\ \left(\left(\frac{-N}{6m^4} - \frac{N}{30m^2} + \frac{3}{280}\right) + \left(\frac{-N}{40m^4} - \frac{N}{168m^2} + \frac{11}{6480}\right) \frac{(\mu+M)}{(2-N)}\right) + B_rN_t \times \\ \left(\left(\frac{-288N}{m^6} - \frac{24N}{m^4} - \frac{3N}{4m^2} + \frac{19}{80}\right) + \left(\frac{-48N}{m^6} - \frac{9N}{2m^4} - \frac{3N}{20m^2} + \frac{1}{32}\right) \frac{(\mu+M)}{(2-N)}\right)\right)\right) \right] dz. \end{split}$$

The normal artery's flow resistance is represented by,

$$\lambda_n = \frac{\Delta p_n}{q},$$

$$\begin{split} \lambda_n &= \frac{-1}{q} \int_0^1 \left[ \frac{\sin{[\alpha]}}{F} + \left( \frac{1}{\left( \frac{N}{2m} \frac{I_0(m)}{I_1(m)} - \frac{N}{m} - \frac{1}{4} \right) + \left( \frac{N}{m} \frac{I_0(m)}{I_1(m)} \frac{1}{8} - \frac{N}{2m} - \frac{N}{m} \frac{I_2(m)}{I_1(m)} - \frac{1}{24} \right) \left( \frac{\frac{\mu}{\kappa} + M}{(2-N)} \right) \right) \\ &\times \left( \frac{q (2-N)}{(1-N)} + \left( \left( \frac{N}{2m} \frac{I_0(m)}{I_1(m)} - \frac{2N}{m} \right) + \left( \frac{N}{m} \frac{I_0(m)}{I_1(m)} \frac{1}{4} - \frac{N}{m} - \frac{2N}{m} \frac{I_2(m)}{I_1(m)} \right) \left( \frac{\mu}{(2-N)} \right) \right) \\ &\times \left( G_r \left( N_b - N_t \right) \left( \frac{1}{32m^2} - \frac{1}{256} \right) - G_r N_b \left( \frac{1}{2m^4} + \frac{1}{6m^2} - \frac{1}{60} \right) - \frac{G_r N_t \left( N_b^2 + N_t^2 \right)}{36864} \right) \\ &\times \left( \frac{7372800}{m^{10}} + \frac{37248}{m^6} + \frac{624}{m^4} + \frac{7}{24} + \frac{921600}{m^8} \right) - \frac{B_r N_t}{N_b} \left( \frac{1}{2m^2} - \frac{1}{16} \right) + B_r N_t \left( \frac{1}{2m^4} + \frac{1}{6m^2} - \frac{1}{60} \right) \right) \\ &- \frac{1}{60} + \frac{B_r \left( N_b^2 + N_t^2 \right)}{36864} \left( \frac{N_t}{N_b} \right) \left( \frac{1152}{m^6} + \frac{144}{m^4} + \frac{6}{m^2} - \frac{3}{8} \right) + \left( G_r \left( N_b - N_t \right) \left( \left( -\frac{N}{128m^2} + \frac{379}{1536} \right) + \left( \frac{755}{12288} \right) \frac{\left( \frac{\mu}{k} + M \right)}{(2-N)} \right) - G_r N_b \left( \left( -\frac{N}{6m^4} - \frac{N}{30m^2} + \frac{3}{280} \right) + \left( \frac{-N}{40m^4} - \frac{N}{168m^2} + \frac{11}{6480} \right) \frac{\left( \frac{\mu}{k} + M \right)}{(2-N)} \right) \\ &- \frac{G_r N_t \left( N_t^2 + N_b^2 \right)}{36864} \left( \left( \left( -\frac{1843200N}{m^{10}} - \frac{153600N}{m^8} - \frac{2255N}{1920} - \frac{24N}{48m^2} + \frac{7N}{768} - \frac{73}{210} \right) + \\ &- \left( \frac{-307200N}{m^{10}} - \frac{28800N}{m^8} - \frac{912N}{66m^4} - \frac{65N}{6m^4} + \frac{27N}{280m^2} - \frac{59}{1920} \right) \frac{\left( \frac{\mu}{k} + M \right)}{(2-N)} + B_r N_t \times \\ &- \left( \left( -\frac{N}{6m^4} - \frac{N}{30m^2} + \frac{3}{280} \right) + \left( \frac{-N}{40m^4} - \frac{N}{168m^2} + \frac{11}{6480} \right) \frac{\left( \frac{\mu}{k} + M \right)}{(2-N)} + B_r N_t \times \\ &- \left( \left( -\frac{288N}{6m^6} - \frac{24N}{m^4} - \frac{3N}{280} \right) + \left( \frac{-N}{40m^4} - \frac{N}{168m^2} + \frac{11}{6480} \right) \frac{\left( \frac{\mu}{k} + M \right)}{(2-N)} + B_r N_t \times \\ &- \left( \left( \frac{-288N}{m^6} - \frac{24N}{m^4} - \frac{3N}{4m^2} + \frac{19}{80} \right) + \left( \frac{-48N}{m^6} - \frac{9N}{2m^4} - \frac{3N}{20m^2} + \frac{1}{32} \right) \frac{\left( \frac{\mu}{k} + M \right)}{(2-N)} \right) \right) \right] dz. \end{split}$$

The normalized flow resistance denoted by,

$$\bar{\lambda} = \frac{\lambda}{\lambda_n}.\tag{34}$$

Dimensionless shear stresses can be determine as follows,

$$\tau_{rz} = \frac{1}{(1-N)} \frac{\partial w}{\partial r} + \frac{N}{(1-N)} V_{\theta}, \tag{35}$$

$$\tau_{zr} = \frac{\partial w}{\partial r} - \frac{1}{(1-N)} V_{\theta},\tag{36}$$

$$\tau_{h} = \tau_{rz} = \frac{r}{2} \left( \frac{dp}{dz} - \frac{\sin \alpha}{F} \right) - \left[ G_{r} \left( \frac{1}{64} \left( N_{b} - N_{t} \right) \left( \frac{r^{3}}{4} - \frac{h^{2}r}{2} \right) - \left( \frac{1}{18} N_{b} \left( \frac{r^{4}}{5} - \frac{h^{3}r}{2} \right) + \frac{N_{t} \left( N_{t}^{2} + N_{b}^{2} \right)}{36864} \left( \frac{r^{11}}{12} - \frac{r^{5}h^{6}}{6} - \frac{r^{7}h^{4}}{8} + \frac{rh^{10}}{2} \right) \right) \right) + B_{r} \left( \frac{-1}{4} \left( \frac{r^{3}}{4} - \frac{h^{2}r}{2} \right) \frac{N_{t}}{N_{b}} + \frac{N_{t}}{N_{b}} \left( \frac{N_{b}}{18} \left( \frac{r^{4}}{5} - \frac{h^{3}r^{2}}{2} \right) + \frac{\left( N_{b}^{2} + N_{t}^{2} \right)}{36864} \left( \frac{r^{7}}{8} - \frac{h^{6}r}{2} \right) \right) \right) \right] + \left( \frac{\mu}{k} + M \right) \frac{wr}{2(1 - N)}, \quad (37)$$

$$\begin{split} \tau_{zr} &= \frac{-N\left(2-N\right)r}{\left(1-N\right)} C_{2}\left(z\right) I_{1}\left(mr\right) + \frac{r}{2} \left(\frac{dP}{dz} - \frac{\sin\alpha}{F}\right) - G_{r}\left(N_{b} - N_{t}\right) \left(\frac{Nr}{32m^{2}} - \frac{h^{2}r}{128} + \frac{r^{3}}{256}\right) \\ &+ G_{r}N_{b} \left(\frac{N}{2m^{4}} - \frac{rh^{3}}{36} + \frac{Nr^{2}}{6m^{2}} + \frac{r^{4}}{90}\right) + \frac{G_{r}N_{t}\left(N_{b}^{2} + N_{t}^{2}\right)}{36864} \left(\frac{7372800Nr}{m^{10}} - \frac{1152Nh^{4}r}{m^{6}}\right) \\ &- \frac{32Nh^{6}r}{m^{4}} + \frac{921600r^{3}}{m^{8}} - \frac{144Nh^{4}r^{3}}{m^{4}} - \frac{4Nh^{6}r^{3}}{m^{2}} + \frac{38400Nr^{5}}{m^{6}} - \frac{6Nh^{4}r^{5}}{m^{2}} + \frac{800Nr^{7}}{m^{4}} \\ &+ \frac{10Nr^{9}}{m^{2}} - \frac{h^{4}r^{7}}{8} - \frac{h^{6}r^{5}}{6} + \frac{h^{10}r}{2} + \frac{r^{11}}{12}\right) + \frac{B_{r}N_{t}}{N_{b}} \left(\frac{Nr}{2m^{2}} - \frac{rh^{2}}{8} + \frac{r^{3}}{16}\right) - B_{r}N_{t} \left(\frac{N}{2m^{4}}\right) \\ &- \frac{rh^{3}}{36} + \frac{Nr^{2}}{6m^{2}} + \frac{r^{4}}{90}\right) - \frac{B_{r}\left(N_{b}^{2} + N_{t}^{2}\right)}{36864} \left(\frac{N_{t}}{N_{b}}\right) \left(\frac{1152Nr}{m^{6}} + \frac{144Nr^{3}}{m^{4}} + \frac{6Nr^{5}}{m^{2}} - \frac{h^{6}r}{2} + \frac{r^{7}}{8}\right) \\ &+ \frac{wr}{2\left(1-N\right)} \left(\frac{\mu}{k} + M\right), \end{split} \tag{38}$$

$$C_{2} = \frac{1}{I_{1}\left(mh\right)} \left[\frac{\left(1-N\right)}{\left(2-N\right)} \left(\frac{dP}{dz} - \frac{\sin\alpha}{F}\right) \frac{h}{2} - \frac{\left(1-N\right)}{\left(2-N\right)} \left(G_{r}\left(N_{b} - N_{t}\right) \left(\frac{h}{2m^{2}} - \frac{h^{3}}{256}\right) - G_{r}N_{b} \times \\ \left(\frac{1}{2m^{4}} + \frac{h^{2}}{6m^{2}} - \frac{h^{4}}{60}\right) - \frac{G_{r}N_{b}\left(N_{b}^{2} + N_{t}^{2}\right)}{36864} \left(\frac{7372800h}{m^{10}} + \frac{921600h^{3}}{m^{8}} + \frac{37248h^{5}}{m^{6}} + \frac{624h^{7}}{m^{4}} + \frac{7h^{11}}{24}\right) - \frac{B_{r}N_{t}}{N_{b}} \left(\frac{h}{2m^{2}} - \frac{h^{3}}{16}\right) + B_{r}N_{t} \left(\frac{1}{2m^{4}} + \frac{h^{2}}{6m^{2}} - \frac{h^{4}}{60}\right) + \frac{B_{r}\left(N_{b}^{2} + N_{t}^{2}\right)}{36864} \frac{N_{t}}{N_{b}} \times \\ \left(\frac{1152h}{m^{6}} + \frac{144h^{3}}{m^{4}} + \frac{6h^{5}}{m^{2}} - \frac{3h^{7}}{8}\right)\right)\right]. \tag{39}$$

# 4 Results and Discussion

The pressure drop, flow resistance, and wall shear stress are represented by (30), (34) and (37), respectively. The impact of various flow parameters on flow impandance, velocity profiles and shear stress have been analysed. Mathematica is used to generate all graphs, by taking:

$$d=0.2, \quad L=1, \quad B_1=0.7, \quad q=0.3, \quad F=0.3, \quad B=1, \quad N=0.1, \quad L_0=0.4,$$
  $\alpha=\frac{\pi}{6}, \quad G_r=0.2, \quad B_r=0.3, \quad N_t=0.8, \quad N_b=0.3, \quad K=0.05, \quad \beta=0.01.$ 

From Figures 2–9, it is observed that when heights of the stenosis increases, the flow resistance also increases because the height of the stenosis increases it disturbs flow pattern and velocity of the fluid decreases and the resistance to the flow increases.

It is also noticed from Figures 2–9 that, the flow resistance  $(\bar{\lambda})$  also increases with various parameters like Inclination  $(\alpha)$ , Magnetic parameter (M), Permeability of porous medium (k), Local temperature Grashof number  $(G_r)$ , Thermophoresis parameter  $(N_t)$  and Local nano-particle Grashof number  $(B_r)$  but decreases with Brownian motion parameter  $(N_b)$  and The Porous medium's permeability (k).

From Figure 8, it is interesting to note that the resistance to the flow increases with increase in Magnetic parameter (M), However, it is noticed that this increase is significant only when the height of the stenosis  $(\delta)$  exceeds the value 0.05. Similarly, with rise of local temperature Grashof number  $(G_r)$ , the resistance to the flow increased Figure 5 i.e when nano fluid particles involved in motion of the fluid particles, buoyance forces are dominated the viscous forces because of temperature variations.

From Figure 7, it is interesting to notice that the resistance to the flow increases with height of the stenosis and permeability (k). This increase is significant when height of the stenosis  $(\delta)$  exceeds the value 0.03. i.e, in small arties, the permeability effect is less when compared with the deposition of plaques.

From Figures 6 and 9, it is observed that the resistance to the flow increases with Brownian motion parameter and viscosity i.e, when collision between molecules reduces the velocity of the fluid, it causes the flow resistance increases. While permeability impacts the ease of blood flow through porous tissues. By controlling these parameters, blood flow can be optimized, especially in systems like vascular networks or drug delivery systems.

Applying a magnetic field in the flow phenomena and the heights of the stenoses increases, the resistance also increases. However, by adjusting the magnetic field appropriately, it becomes possible to control blood pressure and improve conditions such as poor circulation.

The nano fluid particles are involved in the motion of the fluid. These nano fluid particles will enhance the thermal properties (i.e), collision between the molecules increases, but the resistance of the flow increases. The local nanoparticle Grashof number is linked to buoyancy effects caused by temperature variations, while permeability impacts the ease of blood flow through porous tissues. By controlling these parameters, blood flow can be optimized, especially in systems like vascular networks or drug delivery systems.

Figures 10–16 demonstrate the effect of velocity profiles for different values of Brownian motion number  $(N_b)$ , Local temperature Grashof number  $(G_r)$ , Thermophoresis parameter  $(N_t)$ , Local Nanoparticle Grashof number  $(B_r)$ , Magnetic parameter (M), Viscosity  $(\mu)$  and Permeability of porous medium (k).

It is noted that the velocity profiles increase with the increase of Local nanoparticle Grashof number  $(B_r)$ , Local temperature Grashof number  $(G_r)$ , Thermophoresis parameter  $(N_t)$ , Permeability of porous medium (k) but decreases with the increasing of Magnetic parameter (M), Brownian motion parameter  $(N_b)$ . It is interesting to observe that, the effect velocity profile with the increase of Viscosity  $(\mu)$  is decreasing in the region -0.5 to 0.5 and increasing in the other region.

Figures 17–24 demonstrates the effects of height of the stenoses  $(\delta)$  on the wall shear stress  $(\tau_h)$  for different values of Brownian motion number  $(N_b)$ , local temperature Grashof number  $(G_r)$ , Thermophoresis parameter  $(N_t)$ , Local nanoparticle Grashof number  $(B_r)$ , Magnetic parameter (M), Inclination  $(\alpha)$ , and The porous medium's permeability (k).

It is noticed that the Local temperature Grashof number  $(G_r)$ , Local nanoparticle Grashof number  $(B_r)$  and decrease with the wall shear stress  $(\tau_h)$  and Brownian motion parameter  $(N_b)$ , Inclination  $(\alpha)$ , Permeability of porous medium (k), increases with the wall shear stress  $(\tau_h)$ .

The effects of the Magnetic parameter (M), Thermophoresis parameter  $(N_t)$ , and Viscosity  $(\mu)$  help reduce wall shear stress, which can be beneficial in systems where excessive shear stress could cause damage. This is particularly important in the human circulatory system and in sensitive microfluidic devices, where maintaining optimal shear stress is crucial for preventing harm to tissues and ensuring efficient fluid flow.

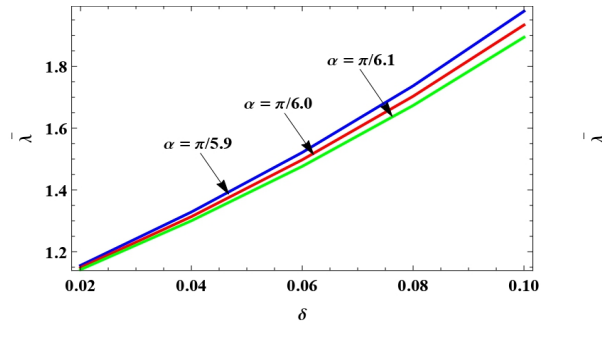


Figure 2: Effect of  $\delta$  on  $\bar{\lambda}$  with  $\alpha$  varying.

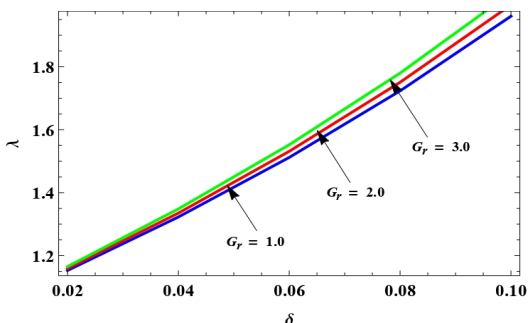


Figure 3: Effect of  $\delta$  on  $\bar{\lambda}$  with  $G_r$  varying.

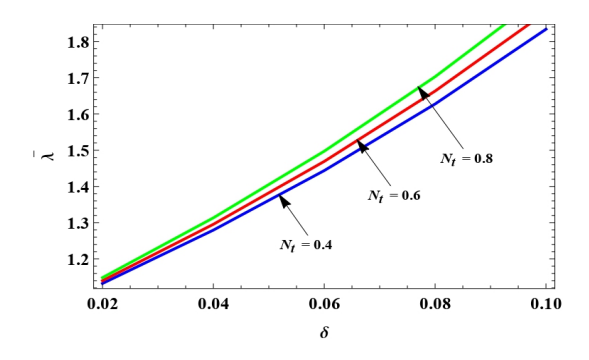


Figure 4: Effect of  $\delta$  on  $\bar{\lambda}$  with  $N_t$  varying.

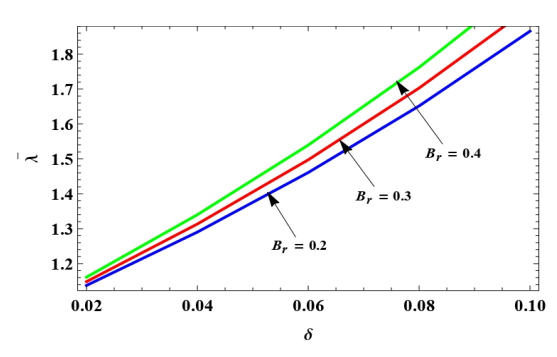


Figure 5: Effect of  $\delta$  on  $\bar{\lambda}$  with  $B_r$  varying.

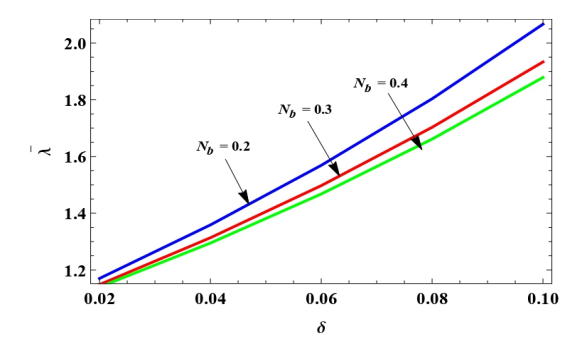


Figure 6: Effect of  $\delta$  on  $\bar{\lambda}$  with  $N_b$  varying.

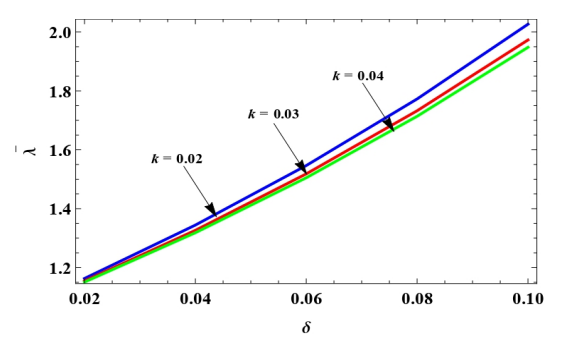


Figure 7: Effect of  $\delta$  on  $\bar{\lambda}$  with k varying.

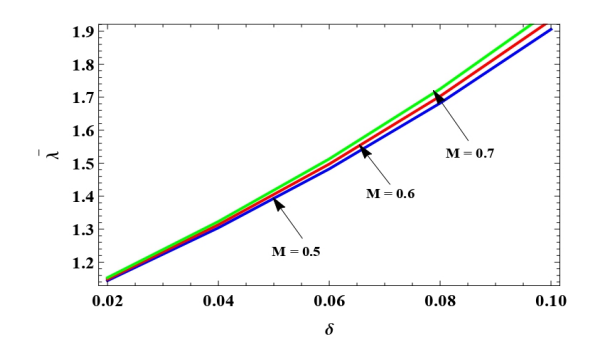


Figure 8: Effect of  $\delta$  on  $\bar{\lambda}$  with M varying.

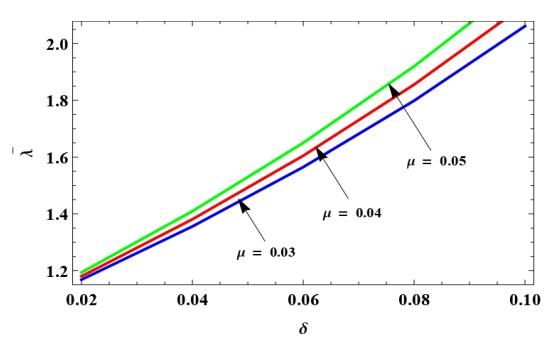


Figure 9: Effect of  $\delta$  on  $\bar{\lambda}$  with  $\mu$  varying.

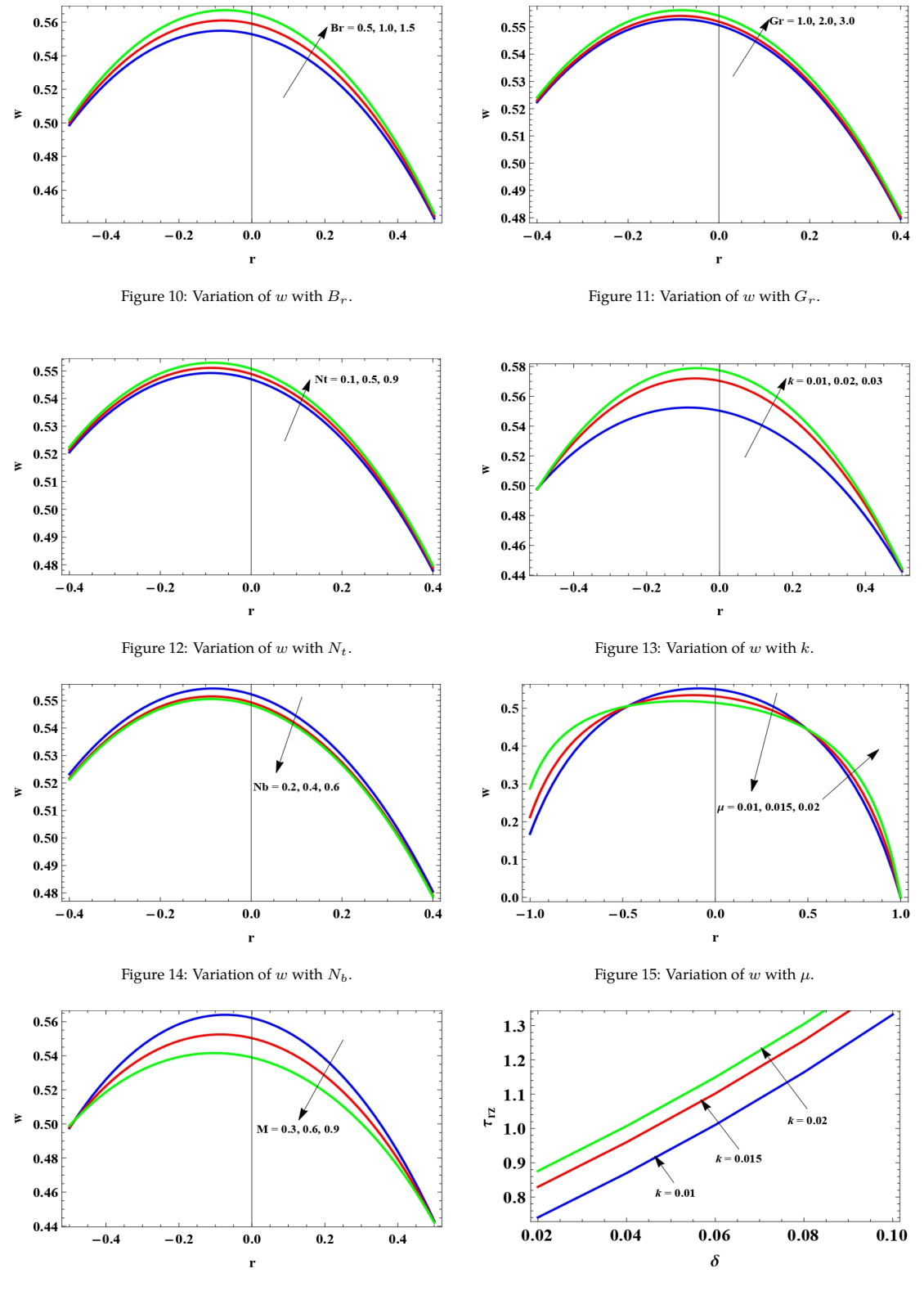


Figure 16: Variation of w with M.

Figure 17: Effect of  $\delta$  on  $\tau_h$  with k varying.

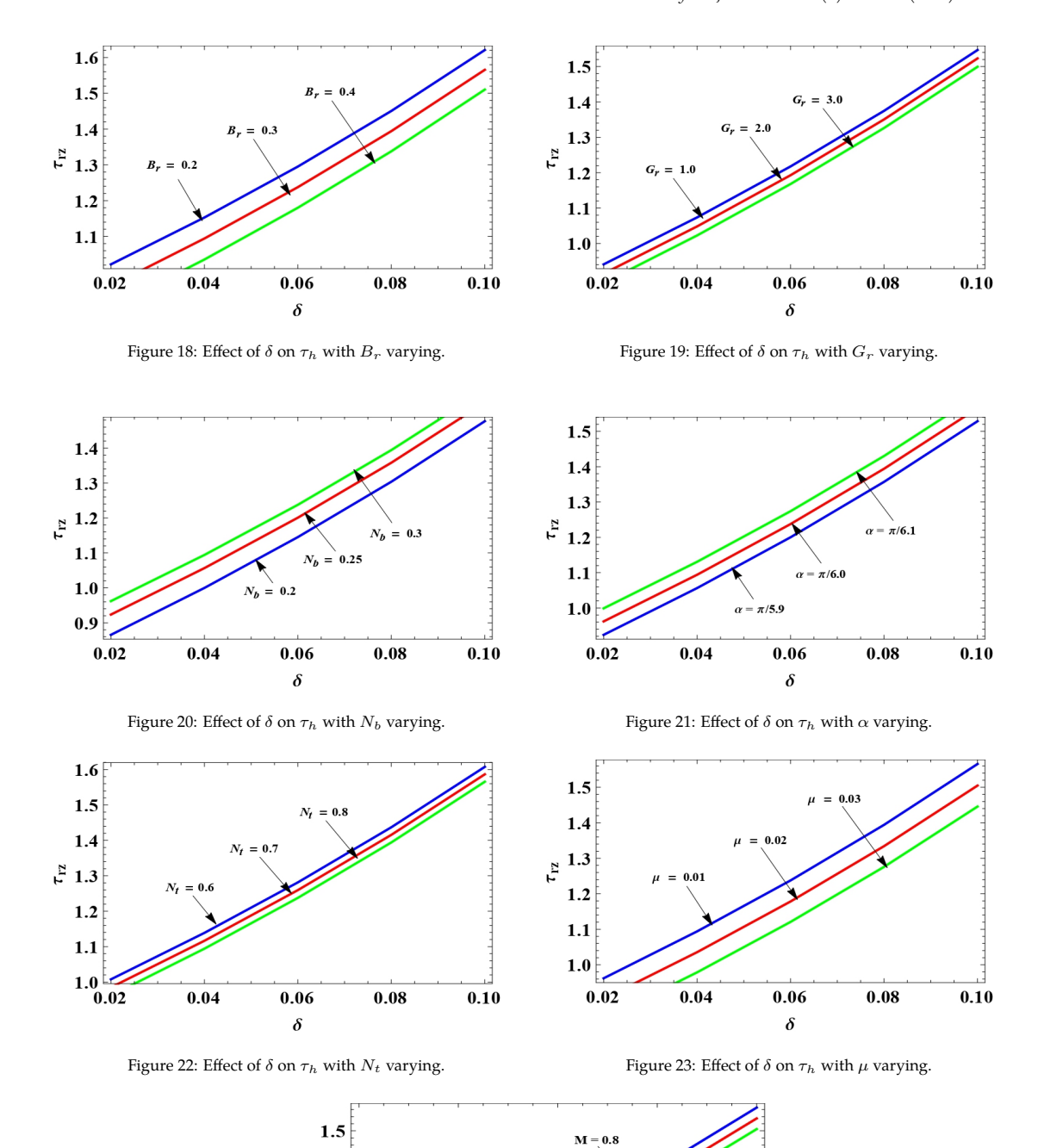


Figure 24: Effect of  $\delta$  on  $\tau_h$  with M varying.

0.06

δ

0.08

0.10

0.04

1.4

1.2 1.1 1.0 0.02 Figures 25–26 displays the streamlines for various values of the magnetic parameter (M), permeability of porous medium (k). It is seen that, the streamlines in the middle are becoming widen, it shows that the blood velocity is increasing and these reduces the resistance to flow decreases with the increase in values of  $M,\ k$ .

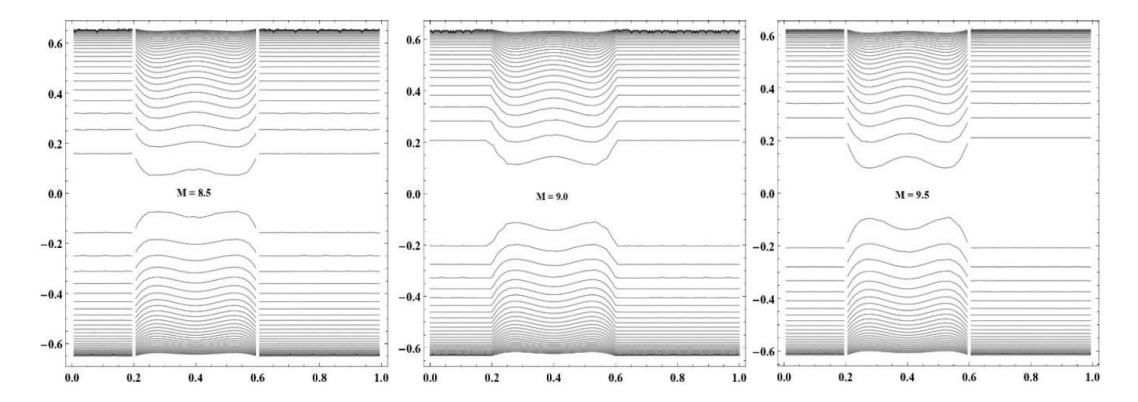


Figure 25: Streamlines for  $M=8.5,\ 9.0\ and\ 9.5$ 

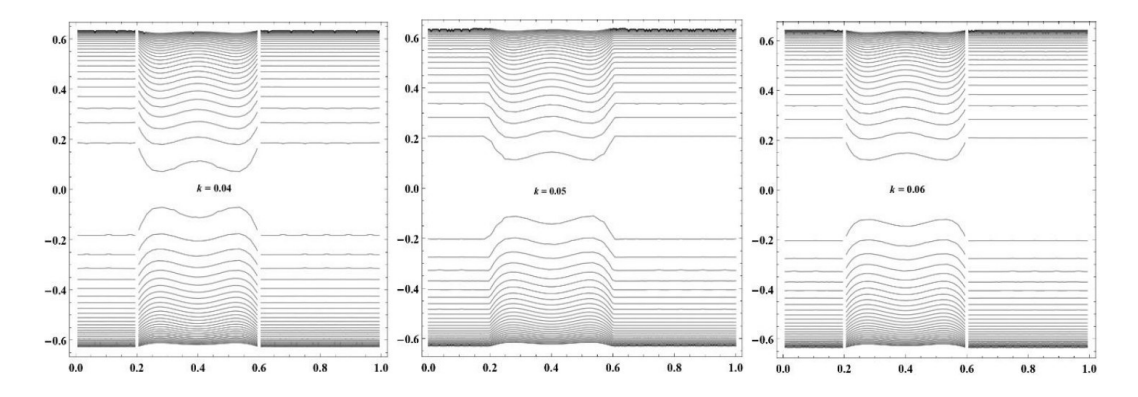


Figure 26: . Streamlines for  $k=0.04,\ 0.05\ and\ 0.06.$ 

## 5 Conclusions

The influence of magnetic filed on a micropolar fluid through an inclined porous medium with overlapping stenoses has been studied. It was possible to evaluate the impact of various factors with different stenosis heights on the flow impandance and shear stress at the wall by finding solutions to the flow characteristic expressions.

#### The observations are:

- The Magnetic parameter, Local nanoparticle Grashof number, Thermophoresis parameter, Local temperature Grashof number increases with flow resistance.
- The axial velocity profiles increase for with the increase of Local nanoparticle Grashof number, Local temperature Grashof number, Thermophoresis parameter, Permeability of porous medium but decreases with the increasing of Brownian motion parameter.

- It is identified that the effect of velocity profile with the increase of Viscosity ( $\mu$ ) is decreasing in the region -0.5 to 0.5 and increasing in the other region.
- The study concludes that varying the intensity of the external magnetic field allows for the regulation of blood flow and shear stress, which can be tailored to desirable levels. This insight can have important clinical applications, particularly in the management and treatment of cardiovascular diseases such as hypertension, high blood pressure, and atherosclerosis. By controlling the magnetic field, it may be possible to reduce the harmful effects of these diseases by controlling blood flow and the forces acting on blood vessel walls.
- The stream lines gradually narrow as the Magnetic parameter (M) and the Permeability of the porous medium (k) increase.
- In addition to the existing findings, we propose several potential extensions to this work. First, the problem could be extended by considering a curved tube geometry, which would more accurately depict flow conditions in systems having curved channels, such heat exchangers or blood vessels.
- The present study considers overlapping stenoses in a simplified form. More complex and
  inconsistent stenosis patterns that may be found in actual biological or engineering systems
  could be the subject of future studies. Deeper understanding of the behavior of nanofluids
  under stenotic conditions may be possible with the model's incorporation of hybrid nanoparticles.

**Acknowledgement** We acknowledge and thank the reviewers and publishers for their valuable comments which help us to enrich the quality of this paper.

**Conflicts of Interest** The authors declare that there are no conflicts of interest.

# References

- [1] I. Abdullah & N. Amin (2010). A micropolar fluid model of blood flow through a tapered artery with a stenosis. *Mathematical Methods in The Applied Sciences*, 33(16), 1910–1923. https://doi.org/10.1002/mma.1303.
- [2] N. S. Akbar, S. U. Rahman, R. Ellahi & S. Nadeem (2014). Nano fluid flow in tapering stenosed arteries with permeable walls. *International Journal of Thermal Sciences*, 85, 54–61. https://doi.org/10.1016/j.ijthermalsci.2014.06.009.
- [3] W. F. W. Azmi, A. Q. Mohamad, L. Y. Jiann & S. Shafie (2024). Mathematical fractional analysis on blood casson fluid in slip and small arteries with the cholesterol porosity effect. *Malaysian Journal of Mathematical Sciences*, *18*(4), 755–774. https://doi.org/10.47836/mjms. 18.4.05.
- [4] R. Bali & U. Awasthi (2007). Effect of a magnetic field on the resistance to blood flow through stenotic artery. *Applied Mathematics and Computation*, 188(2), 1635–1641. https://doi.org/10.1016/j.amc.2006.11.019.
- [5] S. Bilal, S. Akram, M. Athar, K. Saeed, A. Razia & A. Riaz (2024). Numerical analysis on theoretical model of magneto-Williamson nanofluid in relation to viscous dissipation, double-diffusion convection, thermal radiation and multiple slip boundaries. *Pramana*, 98(3), Article ID: 125. https://doi.org/10.1007/s12043-024-02798-z.

- [6] G. R. Charya (1977). Flow of micropolar fluid through a constricted channel. *International Journal of Engineering Science*, 15(12), 719–725. https://doi.org/10.1016/0020-7225(77) 90022-2.
- [7] P. Chaturani & R. P. Samy (1986). Pulsatile flow of Casson's fluid through stenosed arteries with applications to blood flow. *Biorheology*, 23(5), 499–511. https://doi.org/10.3233/bir-1986-23506.
- [8] S. U. Choi & J. A. Eastman. Enhancing thermal conductivity of fluids with nanoparticles. Technical report Argonne National Lab. (ANL), Argonne, IL (United States) 1995.
- [9] I. J. D. Craig & P. G. Watson (2003). Magnetic reconnection solutions based on a generalized Ohm's law. *Solar Physics*, 214, 131–150. https://doi.org/10.1023/A:1024075416016.
- [10] R. Ellahi, S. U. Rahman, M. M. Gulzar, S. Nadeem & K. Vafai (2014). A mathematical study of non-Newtonian micropolar fluid in arterial blood flow through composite stenosis. *Applied Mathematics & Information Sciences*, 8(4), Article ID: 1567. https://doi.org/10.12785/amis/080410.
- [11] A. C. Eringen (1966). Theory of micropolar fluids. *Journal of Mathematics and Mechanics*, 6(1), 1–18.
- [12] J. H. He (2000). A coupling method of a homotopy technique and a perturbation technique for non-linear problems. *International Journal of Non-Linear Mechanics*, 35(1), 37–43. https://doi.org/10.1016/s0020-7462(98)00085-7.
- [13] J. H. He (2005). Application of homotopy perturbation method to nonlinear wave equations. *Chaos, Solitons & Fractals, 26*(3), 695–700. https://doi.org/10.1016/j.chaos.2005.03.006.
- [14] M. A. Ikbal, S. Chakravarty, K. K. L. Wong, J. Mazumdar & P. K. Mandal (2009). Unsteady response of non-Newtonian blood flow through a stenosed artery in magnetic field. *Journal of Computational and Applied Mathematics*, 230(1), 243–259. https://doi.org/10.1016/j.cam.2008. 11.010.
- [15] Y. Khan, S. Akram, M. Athar, K. Saeed, T. Muhammad, A. Hussain, M. Imran & H. A. Alsulaimani (2022). The role of double-diffusion convection and induced magnetic field on peristaltic pumping of a Johnson–Segalman nanofluid in a non-uniform channel. *Nanomaterials*, 12(7), Article ID: 1051. https://doi.org/10.3390/nano12071051.
- [16] J. S. Lee & Y. C. Fung (1970). Flow in locally constricted tubes at low Reynolds numbers. *Journal of Applied Mechanics*, 37(1), 9–16. https://doi.org/10.1115/1.3408496.
- [17] S. N. Majhi & V. R. Nair (1994). Pulsatile flow of third grade fluids under body acceleration—modelling blood flow. *International Journal of Engineering Science*, 32(5), 839–846. https://doi.org/10.1016/0020-7225(94)90064-7.
- [18] P. K. Mandal (2005). An unsteady analysis of non-Newtonian blood flow through tapered arteries with a stenosis. *International Journal of Non-Linear Mechanics*, 40(1), 151–164. https://doi.org/10.1016/j.ijnonlinmec.2004.07.007.
- [19] K. S. Mekheimer & M. El Kot (2007). The micropolar fluid model for blood flow through a stenotic arteries. *International Journal of Pure and Applied Mathematics*, 36(4), Article ID: 393.
- [20] K. S. Mekheimer & M. E. Kot (2008). The micropolar fluid model for blood flow through a tapered artery with a stenosis. *Acta Mechanica Sinica*, 24(6), 637–644. https://doi.org/10. 1007/s10409-008-0185-7.

- [21] J. C. Misra, A. Sinha & G. C. Shit (2011). Mathematical modeling of blood flow in a porous vessel having double stenoses in the presence of an external magnetic field. *International Journal of Biomathematics*, 4(2), 207–225. https://doi.org/10.1142/S1793524511001428.
- [22] K. M. Prasad, B. Vijaya & C. Umadevi (2014). A mathematical model of Herschel–Bulkley fluid through an overlapping stenosis. *IOSR Journal of Mathematics*, 10, 41–46. https://doi.org/10.9790/5728-10224146.
- [23] K. M. Prasad & P. R. Yasa (2020). Flow of non-Newtonian fluid through a permeable artery having non-uniform cross section with multiple stenosis. *Journal of Naval Architecture and Marine Engineering*, 17(1), 31–38. https://doi.org/10.3329/jname.v17i1.40942.
- [24] K. M. Prasad & P. R. Yasa (2021). Micropolar fluid flow in tapering stenosed arteries having permeable walls. *Malaysian Journal of Mathematical Sciences*, 15(1), 157–171.
- [25] G. Radhakrishnamacharya & P. S. Rao (2007). Flow of a magnetic fluid through a non uniform wavy tube. In *Proceedings of the National Academy of Sciences, India. Section A. Physical Sciences*, volume 77 pp. 241–245. Natl Acad Sciences India, Allahabad.
- [26] J. B. Shukla, R. S. Parihar & B. R. P. Rao (1980). Effects of stenosis on non-Newtonian flow of the blood in an artery. *Bulletin of Mathematical Biology*, 42, 283–294. https://doi.org/10.1007/bf02460787.
- [27] T. Sochi (2010). Non-Newtonian flow in porous media. *Polymer*, *51*(22), 5007–5023. https://doi.org/10.1016/j.polymer.2010.07.047.
- [28] V. K. Sud, G. S. Sekhon & R. K. Mishra (1977). Pumping action on blood by a magnetic field. *Bulletin of Mathematical Biology*, *39*, 385–390. https://doi.org/10.1007/bf02462917.
- [29] V. K. Tanwar, N. K. Varshney & R. Agarwal (2014). Effect of porous medium on blood flow through an artery with mild stenosis under the influence of transverse magnetic field. *International Journal of Mathematics*, *5*, 181–188.
- [30] M. N. Uddin & M. A. Alim (2017). Numerical study of blood flow through symmetry and non-symmetric stenosis artery under various flow rates. *IOSR Journal of Dental and Medical Sciences*, *16*(6), 106–115. https://doi.org/10.9790/0853-160601106115.
- [31] K. Vajravelu, S. Sreenadh & V. R. Babu (2005). Peristaltic transport of a Herschel–Bulkley fluid in an inclined tube. *International Journal of Non-Linear Mechanics*, 40(1), 83–90. https://doi.org/10.1016/j.ijnonlinmec.2004.07.001.
- [32] G. Varshney, V. Katiyar & S. Kumar (2010). Effect of magnetic field on the blood flow in artery having multiple stenosis: A numerical study. *International Journal of Engineering, Science and Technology*, 2(2), 967–82. https://doi.org/10.4314/ijest.v2i2.59142.
- [33] H. Yasmin, S. Akram, M. Athar, K. Saeed, A. Razia & J. G. Al Juaid (2024). Impact of multiple slips on thermally radiative peristaltic transport of Sisko nanofluid with double diffusion convection, viscous dissipation, and induced magnetic field. *Nanotechnology Reviews*, 13(1), Article ID: 20240004. https://doi.org/10.1515/ntrev-2024-0004.
- [34] D. Young (1968). Effect of a time-dependent stenosis on flow through a tube. *Journal of Engineering for Industry*, 90(2), 248–254. https://doi.org/10.1115/1.3604621.
- [35] A. Zeeshan, A. Riaz, A. Javaid, T. Nawaz & S. Akram (2024). Effects of tapering and electroosmosis on copper-suspended nanofluid through a composite stenosed artery with permeable walls: Exact solutions. *Brazilian Journal of Physics*, 54(5), Article ID: 195. https://doi.org/10.1007/s13538-024-01576-x.